Structural Engineering and Mechanics, Vol. 19, No. 1 (2005) 73-96 73
DOI: http://dx.doi.org/10.12989/sem.2005.19.1.073

Exact dynamic element stiffness matrix of shear deformable non-symmetric curved beams subjected to initial axial force

Nam-Il, Kim† and Moon-Young, Kim‡

Department of Civil and Environmental Engineering, Sungkyunkwan University, Cheoncheon-Dong, Jangan-Ku, Suwon 440-746, S. Korea

(Received March 8, 2004, Accepted August 31, 2004)

Abstract. For the spatially coupled free vibration analysis of shear deformable thin-walled non-symmetric curved beam subjected to initial axial force, an exact dynamic element stiffness matrix of curved beam is evaluated. Firstly equations of motion and force-deformation relations are rigorously derived from the total potential energy for a curved beam element. Next a system of linear algebraic equations are constructed by introducing 14 displacement parameters and transforming the second order simultaneous differential equations into the first order simultaneous differential equations. And then explicit expressions for displacement parameters are numerically evaluated via eigensolutions and the exact 14×14 dynamic element stiffness matrix is determined using force-deformation relations. To demonstrate the accuracy and the reliability of this study, the spatially coupled natural frequencies of shear deformable thin-walled non-symmetric curved beams subjected to initial axial forces are evaluated and compared with analytical and FE solutions using isoparametric and Hermitian curved beam elements and results by ABAQUS's shell elements.

Key words: thin-walled; curved beam; dynamic stiffness matrix; free vibration; shear deformation.

1. Introduction

The vibrational behavior of shear deformable non-symmetric thin-walled curved beam structures is very complex due to the coupling effect of extensional, bending, and torsional deformation. Due to this reason, it is not easy to evaluate exactly the natural frequencies of the spatially coupled thin-walled curved beam with non-symmetric cross section.

Up to the present, the study for the free in-plane vibration of curved beam have been done by considering various parameters such as boundary conditions, shear deformation, rotary inertia, variable curvatures and variable cross sections. Particularly considerable research (e.g., Nieh *et al.* 2003, Eisenberger and Efraim 2001, Howson and Jemah 1999, Huang *et al.* 1998, Tseng *et al.* 1997, Gupta and Howson 1994) was reported on the exact solutions for free in-plane vibration of curved beam. Nieh *et al.* (2003) developed an analytical solution for the free vibration and stability

† Post-Doctoral Fellow
‡ Ph.D., Professor

of elliptic arches subjected to a uniformly distributed vertical static loading by incorporating series solutions and stiffness matrices. Eisenberger and Efraim (2001) presented the exact dynamic stiffness matrix for a circular beam with a uniform cross section. The matrix is derived from the differential equation of motion for a beam. This stiffness matrix is free of membrane and shear locking as the shape functions that are used are the exact solution of the differential equations of motion. Howson and Jemah (1999) evaluated the planar natural frequency of curved Timoshenko beams with uniform cross section and arbitrary boundary conditions. This is achieved by using exact dynamic stiffness matrix and by utilizing a new version of the Wittrick-Williams algorithm (Wittrick and Williams 1971) which determines the number of natural frequencies exceeded by any trial frequency. Huang *et al.* (1998) and Tseng *et al.* (1997) provided the systematic approach to solve the in-plane vibrations of arches with variable cross section and constant cross section, respectively using the Frobenius method (Whittaker and Watson 1965) combined with the dynamic stiffness method. Gupta and Howson (1994) presented a method for converging with certainty upon any required natural frequency of a plane slender curved beam. They used the exact member theory in conjunction with the dynamic stiffness technique and this necessitated the solution of a transcendental eigenvalue problem. Solutions were achieved by use of the Wittrick-Williams algorithm.

Also the research for the free out-of-plane vibration analysis of curved beam has been performed by several authors (Lee and Chao 2001, Huang *et al.* 2000, 1998, Howson and Jemah 1999, Howson *et al.* 1995, Kang *et al.* 1996). Lee and Chao (2001) derived the governing differential equations for the out-of-plane vibrations of a curved non-uniform beam of constant radius via Hamilton's principle. With the explicit relations between the torsional displacement, its derivative and the flexural displacement, the two coupled governing characteristic differential equations are reduced to one sixth order ordinary differential equation with variable coefficients in the out-of-plane flexural displacement. Huang *et al.* (2000, 1998) developed the dynamic stiffness matrix for non-circular curved beams from a series of solution using the Frobenius method, with which an exact solution of the out-of-plane free vibration of this type of beam was derived. Howson and Jemah (1999) and Howson *et al.* (1995) evaluated the required natural frequencies of out-of-plane motion of plane structures composed of Timoshenko and slender curved beams, respectively. The solution of the inherent transcendental eigenvalue problem was achieved through a variation on the Wittrick-Williams algorithm. Kang *et al.* (1996) computed the eigenvalues of free vibration of horizontally curved beams with doubly symmetric cross section using the differential quadrature method (DQM).

On the other hand, the study for free in-plane and out-of-plane decoupled vibration analysis of curved beam have been performed by a few researchers (Yildrim 1997, Kang *et al.* 1996, 1995).

Even though a significant amount of research has been conducted on development of exact solutions for free vibration analysis of curved beam structures, to the author's knowledge, there was no study reported on the exact solutions for the spatially coupled free vibration of shear deformable thin-walled curved beams with non-symmetric cross section in the literature. Recently Kim *et al.* (2004) presented an improved energy formulation for spatially coupled free vibration of shear deformable thin-walled curved beams with non-symmetric cross section and derived an analytical solutions for free out-of-plane vibrations of curved beams with monosymmetric cross section.

The aim of this study is to evaluate the exact dynamic element stiffness matrix of shear deformable non-symmetric thin-walled curved beams subjected to initial axial forces. For this, equations of motion and force-deformation relations are first derived for a curved beam element.

Next the second order simultaneous differential equations are transformed into a set of the first order simultaneous ordinary differential equations by introducing 14 displacement parameters. And then using the solutions of the eigenproblem, displacement functions of 14 displacement parameters are exactly derived with respect to nodal displacements. Finally nodal forces are exactly evaluated using force-deformation relationships and 14 × 14 dynamic element stiffness matrix of curved beams is determined.

Through the numerical examples, the spatially coupled natural frequencies of shear deformable thin-walled curved beam with non-symmetric cross section are evaluated and compared with analytical solutions and the results analyzed using the isoparametric and Hermitian curved beam elements and the ABAQUS's shell elements.

2. Equations of motion of shear deformable curved beam with non-symmetric thin-walled cross sections

To derive the equations of motion of a shear deformable thin-walled curved beam with non-symmetric cross section subjected to intial axial forces, we adopts a global curvilinear coordinate system (x_1, x_2, x_3) as shown in Fig. 1 in which the x_1 axis coincides with a centroid axis but x_2, x_3 axes are not necessarily principal inertia axes. The displacement parameters and the stress resultants of thin-walled curved beams defined at the non-symmetric cross-section are shown in Figs. 2(a) and 2(b), respectively. Where U_x, U_y, U_z and ω_1, ω_2, ω_3 are rigid body translations and rotations of the cross section with respect to x_1, x_2 and x_3 axes, respectively. f is a displacement parameter measuring warping deformations. Stress resultants in Fig. 2(b) are defined by

$$F_1 = \int_A \tau_{11} dA, \quad F_2 = \int_A \tau_{12} dA, \quad F_3 = \int_A \tau_{13} dA, \quad M_1 = \int_A (\tau_{13} x_2 - \tau_{12} x_3) dA$$

$$M_2 = \int_A \tau_{11} x_3 dA, \quad M_3 = -\int_A \tau_{11} x_2 dA, \quad M_\phi = \int_A \tau_{11} \phi dA \tag{1a-g}$$

where F_1, F_2 and F_3 are the axial, shear forces acting at the centroid, M_1, M_2 and M_3 are the total twist moment with respect to the centroid axis, bending moments with respect to x_2 and x_3 axes, respectively. M_ϕ is the bimoment.

Now allowing the shear deformation, the rotary inertia and the thickness-curvature effect, the

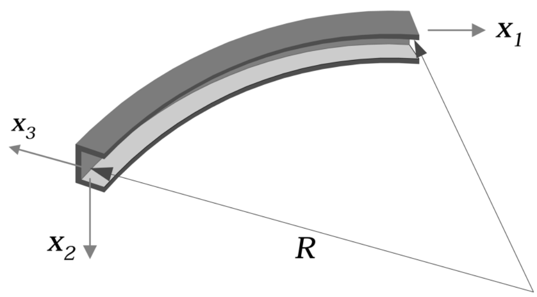

Fig. 1 A curvilinear coordinate system for non-symmetric thin-walled curved beams

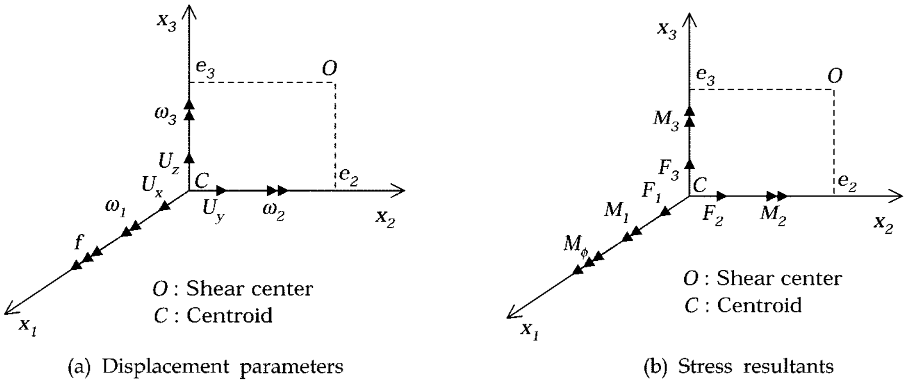

Fig. 2 Notation for displacement parameters and stress resultants

elastic stain and kinetic energies (Kim *et al.* 2004) of thin-walled curved beams with non-symmetric cross section can be written as follows

$$
\begin{aligned}
\Pi_E = \frac{1}{2}\int_0^L \Bigg[& EA\left(U_x' + \frac{U_z}{R}\right)^2 + E\hat{I}_2\left(\omega_2' - \frac{U_x'}{R} - \frac{U_z}{R^2}\right)^2 + E\hat{I}_3\left(\omega_3' - \frac{\omega_1}{R}\right)^2 + E\hat{I}_\phi f'^2 \\
& + 2E\hat{I}_{\phi 2}\left(\omega_2' - \frac{U_x'}{R} - \frac{U_z}{R^2}\right)f' - 2E\hat{I}_{\phi 3}\left(\omega_3' - \frac{\omega_1}{R}\right)f' - 2E\hat{I}_{23}\left(\omega_3' - \frac{\omega_1}{R}\right)\left(\omega_2' - \frac{U_x'}{R} - \frac{U_z}{R^2}\right) \\
& + GJ\left(\omega_1' + \frac{\omega_3}{R}\right)^2 + GA_2(U_y' - \omega_3)^2 + GA_3\left(U_z' - \frac{U_x}{R} + \omega_2\right)^2 + GA_r\left(\omega_1' + \frac{\omega_3}{R} + f\right)^2 \\
& + 2GA_{23}(U_y' - \omega_3)\left(U_z' - \frac{U_x}{R} + \omega_2\right) + 2GA_{2r}(U_y' - \omega_3)\left(\omega_1' + \frac{\omega_3}{R} + f\right) \\
& + 2GA_{3r}\left(U_z' - \frac{U_x}{R} + \omega_2\right)\left(\omega_1' + \frac{\omega_3}{R} + f\right)\Bigg]dx_1
\end{aligned} \tag{2}
$$

and

$$
\begin{aligned}
\Pi_M = \frac{1}{2}\rho\omega^2\int_0^L \Bigg[& A(U_x^2 + U_y^2 + U_z^2) + \tilde{I}_o\omega_1^2 + \tilde{I}_2\omega_2^2 + \tilde{I}_3\omega_3^2 + \tilde{I}_\phi f^2 + 2\frac{I_2}{R}(U_x\omega_2 - U_y\omega_1) \\
& -2\frac{I_{23}}{R}(U_x\omega_3 - U_z\omega_1) - 2\tilde{I}_{23}\omega_2\omega_3 + 2\tilde{I}_{\phi 2}\omega_2 f - 2\tilde{I}_{\phi 3}\omega_3 f + 2\frac{I_{\phi 2}}{R}U_x f\Bigg]dx_1
\end{aligned} \tag{3}
$$

where

$$
\begin{aligned}
&\hat{I}_2 = I_2 - \frac{I_{222}}{R}, \quad \hat{I}_3 = I_3 - \frac{I_{233}}{R}, \quad \hat{I}_\phi = I_\phi - \frac{I_{\phi\phi 2}}{R} \\
&\hat{I}_{\phi 2} = I_{\phi 2} - \frac{I_{\phi 22}}{R}, \quad \hat{I}_{\phi 3} = I_{\phi 3} - \frac{I_{\phi 23}}{R}, \quad \hat{I}_{23} = I_{23} - \frac{I_{223}}{R}
\end{aligned} \tag{4}
$$

$$\tilde{I}_o = I_2 + I_3 + \frac{I_{222} + I_{233}}{R}, \quad \tilde{I}_2 = I_2 + \frac{I_{222}}{R}, \quad \tilde{I}_3 = I_3 + \frac{I_{233}}{R}$$

$$\tilde{I}_{23} = I_{23} + \frac{I_{223}}{R}, \quad \tilde{I}_\phi = I_\phi + \frac{I_{\phi\phi 2}}{R}, \quad \tilde{I}_{\phi 2} = I_{\phi 2} + \frac{I_{\phi 22}}{R}, \quad \tilde{I}_{\phi 3} = I_{\phi 3} + \frac{I_{\phi 23}}{R} \tag{5}$$

where E and G are the Young's modulus and the shear modulus, J and ρ are the torsional constant and the density, respectively. I_2, I_3, I_{23}, I_{222}, I_{223}, I_{233}, I_ϕ, $I_{\phi 2}$, $I_{\phi 3}$, $I_{\phi 22}$, $I_{\phi 23}$, $I_{\phi\phi 2}$ are the sectional constants of which the detailed expressions may be referred to the Reference (Kim *et al.* 2004). The superscript 'prime' denotes the derivative with respect to x_1.

And referring to Kim *et al.* (2000), the potential energy Π_G due to the initial axial force ${}^oF_1$ can be expressed as follows

$$\Pi_G = \frac{1}{2}\int_0^L \left[{}^oF_1 \left\{ U_y'^2 + \left(U_z' - \frac{U_x}{R} \right)^2 \right\} + {}^oF_1 \beta \left(\omega_1' + \frac{\omega_3}{R} \right)^2 \right] dx_1 \tag{6}$$

where

$$\beta = \frac{\hat{I}_2 + \hat{I}_3}{A + \dfrac{\hat{I}_2}{R^2}} \tag{7}$$

In Eq. (6), the ${}^oF_1\beta$ denotes the Wagner effect and the total potential energy Π is can be expressed as

$$\Pi = \Pi_E + \Pi_G - \Pi_M \tag{8}$$

Now, by variation of Eq. (8) with respect to seven displacements, equations of motion, boundary conditions and force-deformation relations for shear deformable curved beam are derived as follows

$$\begin{aligned}
&-EA\left(U_x'' + \frac{1}{R}U_z'\right) + \frac{1}{R}E\hat{I}_2\left(\omega_2'' - \frac{1}{R}U_x'' - \frac{1}{R^2}U_z'\right) + \frac{1}{R}E\hat{I}_{\phi 2}f'' - \frac{1}{R}E\hat{I}_{23}\left(\omega_3'' - \frac{1}{R}\omega_1'\right) \\
&-\frac{1}{R}GA_3\left(U_z' + \omega_2 - \frac{1}{R}U_x\right) - \frac{1}{R}GA_{23}(U_y' - \omega_3) - \frac{1}{R}GA_{3r}\left(\omega_1' + f + \frac{1}{R}\omega_3\right) - {}^oF\left(\frac{1}{R}U_z' - \frac{1}{R^2}U_x\right) \\
&-\rho\omega^2\left(AU_x + \frac{I_2}{R}\omega_2 - \frac{I_{23}}{R}\omega_3 + \frac{I_{\phi 2}}{R}f\right) = 0
\end{aligned}$$

$$\begin{aligned}
&GA_2(U_y'' - \omega_3') + GA_{23}\left(U_z'' + \omega_2' - \frac{1}{R}U_x'\right) + GA_{2r}\left(\omega_1'' + f' + \frac{1}{R}\omega_3'\right) + {}^oF_1U_y'' \\
&+\rho\omega^2\left(AU_y - \frac{I_2}{R}\omega_1\right) = 0
\end{aligned}$$

$$\frac{1}{R}EA\left(U_x' + \frac{1}{R}U_z\right) - \frac{1}{R^2}E\hat{I}_2\left(\omega_2' - \frac{1}{R}U_x' - \frac{1}{R^2}U_z\right) - \frac{1}{R^2}E\hat{I}_{\phi 2}f' + \frac{1}{R^2}E\hat{I}_{23}\left(\omega_3' - \frac{1}{R}\omega_1\right)$$

$$- GA_3\left(U_z'' + \omega_2' - \frac{1}{R}U_x'\right) - GA_{23}(U_y'' - \omega_3') - GA_{3r}\left(\omega_1'' + f' + \frac{1}{R}\omega_3'\right) - {}^oF_1\left(U_z'' - \frac{1}{R}U_x'\right)$$

$$-\rho\omega^2\left(AU_y + \frac{I_{23}}{R}\omega_1\right) = 0$$

$$-\frac{1}{R}E\hat{I}_3\left(\omega_3' - \frac{1}{R}\omega_1\right) + \frac{1}{R}E\hat{I}_{\phi 3}f' + \frac{1}{R}E\hat{I}_{23}\left(\omega_2' - \frac{1}{R}U_x' - \frac{1}{R^2}U_z\right) - GJ\left(\omega_1'' + \frac{1}{R}\omega_3'\right)$$

$$- GA_r\left(\omega_1'' + f' + \frac{1}{R}\omega_3'\right) - GA_{2r}(U_y'' - \omega_3') - GA_{3r}\left(U_z'' + \omega_2' - \frac{1}{R}U_x'\right) - \beta^o F_1\left(\omega_1'' + \frac{1}{R}\omega_3'\right)$$

$$-\rho\omega^2\left(\tilde{I}_o\omega_1 - \frac{I_2}{R}U_y + \frac{I_{23}}{R}U_z\right) = 0$$

$$- E\hat{I}_2\left(\omega_2'' - \frac{1}{R}U_x'' - \frac{1}{R^2}U_z'\right) - E\hat{I}_{\phi 2}f'' + E\hat{I}_{23}\left(\omega_3'' - \frac{1}{R}\omega_1'\right) + GA_3\left(U_z' + \omega_2 - \frac{1}{R}U_x\right)$$

$$+ GA_{23}(U_y' - \omega_3) + GA_{3r}\left(\omega_1' + f + \frac{1}{R}\omega_3\right) - \rho\omega^2\left(\tilde{I}_2\omega_2 + \frac{I_2}{R}U_x - \tilde{I}_{23}\omega_3 + \tilde{I}_{\phi 2}f\right) = 0$$

$$- E\hat{I}_3\left(\omega_3'' - \frac{1}{R}\omega_1'\right) + E\hat{I}_{\phi 3}f'' + E\hat{I}_{23}\left(\omega_2'' - \frac{1}{R}U_x'' - \frac{1}{R^2}U_z'\right) + \frac{1}{R}GJ\left(\omega_1' + \frac{1}{R}\omega_3\right)$$

$$- GA_2(U_y' - \omega_3) - GA_{23}\left(U_z' + \omega_2 - \frac{1}{R}U_x\right) + \frac{1}{R}GA_r\left(\omega_1' + f + \frac{1}{R}\omega_3\right)$$

$$- GA_{2r}\left(\omega_1' + f - \frac{1}{R}U_y' + \frac{2}{R}\omega_3\right) + GA_{3r}\left(U_z' + \omega_2 - \frac{1}{R}U_x\right)\frac{1}{R} + \beta^o F_1\left(\frac{1}{R}\omega_1' + \frac{1}{R^2}\omega_3\right)$$

$$-\rho\omega^2\left(\tilde{I}_3\omega_3 - \frac{I_{23}}{R}U_x - \tilde{I}_{23}\omega_2 - \tilde{I}_{\phi 3}f\right) = 0$$

$$- E\hat{I}_\phi f'' - E\hat{I}_{\phi 2}\left(\omega_2'' - \frac{1}{R}U_x'' - \frac{1}{R^2}U_z'\right) + E\hat{I}_{\phi 3}\left(\omega_3'' - \frac{1}{R}\omega_1'\right) + GA_r\left(\omega_1' + f + \frac{1}{R}\omega_3\right)$$

$$+ GA_{2r}(U_y' - \omega_3) + GA_{3r}\left(U_z' + \omega_2 - \frac{1}{R}U_x\right) - \rho\omega^2\left(\tilde{I}_\phi f + \tilde{I}_{\phi 2}\omega_2 - \tilde{I}_{\phi 3}\omega_2 + \frac{I_{\phi 2}}{R}U_x\right) = 0 \qquad \text{(9a-g)}$$

and

$$\delta U_x(o) = \delta U_x^p \text{ or } F_1(o) = -F_1^p \quad ; \quad \delta U_x(l) = \delta U_x^q \text{ or } F_1(l) = F_1^q \qquad \text{(10a,b)}$$

$$\delta U_y(o) = \delta U_y^p \text{ or } F_2(o) = -F_2^p \quad ; \quad \delta U_y(l) = \delta U_y^q \text{ or } F_2(l) = F_2^q \qquad \text{(10c,d)}$$

$$\delta U_z(o) = \delta U_z^p \text{ or } F_3(o) = -F_3^p \quad ; \quad \delta U_z(l) = \delta U_z^q \text{ or } F_3(l) = F_3^q \qquad \text{(10e,f)}$$

$$\delta\omega_1(o) = \delta\omega_1^p \text{ or } M_1(o) = -M_1^p \quad ; \quad \delta\omega_1(l) = \delta\omega_1^q \text{ or } M_1(l) = M_1^q \qquad \text{(10g,h)}$$

$$\delta\omega_2(o) = \delta\omega_2^p \text{ or } M_2(o) = -M_2^p \quad ; \quad \delta\omega_2(l) = \delta\omega_2^q \text{ or } M_2(l) = M_2^q \tag{10i,j}$$

$$\delta\omega_3(o) = \delta\omega_3^p \text{ or } M_3(o) = -M_3^p \quad ; \quad \delta\omega_3(l) = \delta\omega_3^q \text{ or } M_3(l) = M_3^q \tag{10k,l}$$

$$\delta f(o) = \delta f^p \text{ or } M_\phi(o) = -M_\phi^p \quad ; \quad \delta f(l) = \delta f^q \text{ or } M_\phi(l) = M_\phi^q \tag{10m,n}$$

And force-deformation relations are

$$F_1 = EA\left(U_x' + \frac{1}{R}U_z\right) - \frac{1}{R}E\hat{I}_2\left(\omega_2' - \frac{1}{R}U_x' - \frac{1}{R^2}U_z\right) - \frac{1}{R}E\hat{I}_{\phi 2}f' + \frac{1}{R}E\hat{I}_{23}\left(\omega_3' - \frac{1}{R}\omega_1\right) \tag{11a}$$

$$F_2 = GA_2(U_y' - \omega_3) + GA_{23}\left(U_z' + \omega_2 - \frac{1}{R}U_x\right) + GA_{2r}\left(\omega_1' + f + \frac{1}{R}\omega_3\right) + {}^oF_1U_y' \tag{11b}$$

$$F_3 = GA_3\left(U_z' + \omega_2 - \frac{1}{R}U_x\right) + GA_{23}(U_y' - \omega_3) + GA_{3r}\left(\omega_1' + f + \frac{1}{R}\omega_3\right) + {}^oF_1\left(U_z' - \frac{1}{R}U_x\right) \tag{11c}$$

$$\begin{aligned} M_1 = {} & GJ\left(\omega_1' + \frac{1}{R}\omega_3\right) + GA_r\left(\omega_1' + f + \frac{1}{R}\omega_3\right) + GA_{2r}(U_y' - \omega_3) + GA_{3r}\left(U_z' + \omega_2 - \frac{1}{R}U_x\right) \\ & + \beta^oF_1\left(\omega_1' + \frac{1}{R}\omega_3\right) \end{aligned} \tag{11d}$$

$$M_2 = E\hat{I}_2\left(\omega_2' - \frac{1}{R}U_x' - \frac{1}{R^2}U_z\right) + E\hat{I}_{\phi 2}f' - E\hat{I}_{23}\left(\omega_3' - \frac{1}{R}\omega_1\right) \tag{11e}$$

$$M_3 = E\hat{I}_3\left(\omega_3' - \frac{1}{R}\omega_1\right) - E\hat{I}_{\phi 3}f' - E\hat{I}_{23}\left(\omega_2' - \frac{1}{R}U_x' - \frac{1}{R^2}U_z\right) \tag{11f}$$

$$M_\phi = E\hat{I}_\phi f' + E\hat{I}_{\phi 2}\left(\omega_2' - \frac{1}{R}U_x' - \frac{1}{R^2}U_z\right) - E\hat{I}_{\phi 3}\left(\omega_3' - \frac{1}{R}\omega_1\right) \tag{11g}$$

where it should be noted that Eqs. (11b-d) include the effects of the initial axial force.

3. Exact dynamic element stiffness matrix of shear deformable curved beam elements

3.1 Exact evaluation of displacement functions

In order to transform the equations of motion in Eqs. (9a-g) into a set of the first order ordinary differential equations, a displacement state vector composed of 14 displacement parameters is defined by

$$\begin{aligned} \boldsymbol{d}(\boldsymbol{x}) &= \langle d_1, d_2, d_3, d_4, d_5, d_6, d_7, d_8, d_9, d_{10}, d_{11}, d_{12}, d_{13}, d_{14}\rangle^T \\ &= \langle U_x, U_x', U_y, U_y', \omega_3, \omega_3', U_z, U_z', \omega_2, \omega_2', \omega_1, \omega_1', f, f'\rangle^T \end{aligned} \tag{12}$$

Using Eq. (12), Eqs. (9a-g) are transformed into the first order simultaneous ordinary differential equations with constant coefficients.

$$d_1' = d_2 \tag{13a}$$

$$-\left(EA+\frac{E\hat{I}_2}{R^2}\right)d_2' - \frac{GA_{23}}{R}d_3' - \frac{E\hat{I}_{23}}{R}d_6' - \frac{GA_3}{R}d_7' + \frac{E\hat{I}_2}{R}d_{10}' - \frac{GA_{3r}}{R}d_{11}' + \frac{E\hat{I}_{\phi 2}}{R}d_{14}' =$$
$$+\left\{\rho\omega^2 A - \frac{1}{R^2}(GA_3 + {}^oF_1)\right\}d_1 - \left(\frac{GA_{23}}{R} - \frac{GA_{3r}}{R^2} + \rho\omega^2\frac{I_{23}}{R}\right)d_5 + \frac{1}{R}\left(EA + \frac{E\hat{I}_2}{R^2} + {}^oF_1\right)d_8$$
$$+\left(\frac{GA_3}{R} + \rho\omega^2\frac{I_2}{R}\right)d_9 - \frac{E\hat{I}_{23}}{R^2}d_{12} + \left(\frac{GA_{3r}}{R} + \rho\omega^2\frac{I_{\phi 2}}{R}\right)d_{13} \tag{13b}$$

$$d_3' = d_4 \tag{13c}$$

$$(GA_2 + {}^oF_1)d_4' + GA_{23}d_8' + GA_{2r}d_{12}' = \frac{GA_{23}}{R}d_2 - \rho\omega^2 A d_3 + \left(GA_2 - \frac{GA_{2r}}{R}\right)d_6$$
$$- GA_{23}d_{10} + \rho\omega^2\frac{I_2}{R}d_{11} - GA_{2r}d_{14} \tag{13d}$$

$$d_5' = d_6 \tag{13e}$$

$$\frac{1}{R}\left(EA + \frac{E\hat{I}_2}{R^2} + GA_3 + {}^oF_1\right)d_1' - GA_{23}d_4' + \frac{E\hat{I}_{23}}{R^2}d_5' - (GA_3 + {}^oF_1)d_8' - \frac{E\hat{I}_2}{R^2}d_9' - GA_{3r}d_{12}'$$
$$= -\left(GA_{23} - \frac{GA_{3r}}{R}\right)d_6 + \left\{\rho\omega^2 A - \frac{1}{R^2}\left(EA + \frac{E\hat{I}_2}{R^2}\right)\right\}d_7 + GA_3 d_{10} + \left(\frac{E\hat{I}_{23}}{R^3} + \rho\omega^2\frac{I_{23}}{R}\right)d_{11} \tag{13f}$$
$$+\left(GA_{3r} + \frac{E\hat{I}_{\phi 2}}{R^2}\right)d_{14}$$

$$d_7' = d_8 \tag{13g}$$

$$-\frac{1}{R}\left(\frac{E\hat{I}_{23}}{R} - GA_{3r}\right)d_1' - GA_{2r}d_4' - \frac{1}{R}(E\hat{I}_3 + GA_r)d_5' - GA_{3r}d_8' + \frac{E\hat{I}_{23}}{R}d_9' - (GJ + GA_r + \beta^o F_1)d_{12}'$$
$$= -\rho\omega^2\frac{I_2}{R} + \left(\frac{GJ}{R} - GA_{2r} + \frac{\beta_o}{R}F_1\right)d_6 + \left(\frac{E\hat{I}_{23}}{R^3} + \rho\omega^2\frac{I_{23}}{R}\right)d_7 + GA_{3r}d_{10} + \left(\rho\omega^2\tilde{I}_o - \frac{E\hat{I}_3}{R^2}\right)d_{11}$$
$$-\left(\frac{E\hat{I}_{\phi 3}}{R} - GA_r\right)d_{14} \tag{13h}$$

$$d_9' = d_{10} \tag{13i}$$

$$\frac{E\hat{I}_2}{R}d_2' + GA_{23}d_3' + E\hat{I}_{23}d_6' + GA_3d_7' - E\hat{I}_2d_{10}' + GA_{3r}d_{11}' - E\hat{I}_{\phi 2}d_{14}'$$

$$= \left(\frac{GA_3}{R} + \rho\omega^2\frac{I_2}{R}\right)d_1 + \left(GA_{23} - \frac{GA_{3r}}{R} - \rho\omega^2\tilde{I}_{23}\right)d_5 - \frac{E\hat{I}_2}{R^2}d_8 + (\rho\omega^2\tilde{I}_2 - GA_3)d_9 \tag{13j}$$

$$+ \frac{E\hat{I}_{23}}{R}d_{12} + (\rho\omega^2\tilde{I}_{\phi 2} - GA_{3r})d_{13}$$

$$d_{11}' = d_{12} \tag{13k}$$

$$-\frac{E\hat{I}_{23}}{R}d_2' - \left(GA_2 - \frac{GA_{2r}}{R}\right)d_3' - E\hat{I}_3d_6' - \left(GA_{23} - \frac{GA_{3r}}{R}\right)d_7' + E\hat{I}_{23}d_{10}'$$

$$+ \left(\frac{GJ}{R} + \frac{GA_r}{R} - GA_{2r} + \frac{\beta_o}{R}{}^oF_1\right)d_{11}' + E\hat{I}_{\phi 3}d_{14}' = -\left(\frac{GA_{23}}{R} - \frac{GA_{3r}}{R^2} + \rho\omega^2\frac{I_{23}}{R}\right)d_1$$

$$-\left\{\frac{GJ}{R^2} + GA_2 + \frac{GA_r}{R^2} - \frac{2GA_{2r}}{R} + \frac{\beta_o}{R^2}{}^oF_1 - \rho\omega^2\tilde{I}_3\right\}d_5 + \frac{E\hat{I}_{23}}{R^2}d_8 + \left(GA_{23} - \frac{GA_{3r}}{R} - \rho\omega^2\tilde{I}_{23}\right)d_9$$

$$-\frac{E\hat{I}_3}{R}d_{12} - \left(\frac{GA_r}{R} - GA_{2r} + \rho\omega^2\tilde{I}_{\phi 3}\right)d_{13} \tag{13l}$$

$$d_{13}' = d_{14} \tag{13m}$$

$$\frac{E\hat{I}_{\phi 2}}{R}d_2' + GA_{2r}d_3' + E\hat{I}_{\phi 3}d_6' + GA_{3r}d_7' - E\hat{I}_{\phi 2}d_{10}' + GA_rd_{11}' - E\hat{I}_\phi d_{14}'$$

$$= \left(\frac{GA_{3r}}{R} + \rho\omega^2\frac{I_{\phi 2}}{R}\right)d_1 + \left(GA_{2r} - \frac{GA_r}{R} - \rho\omega^2\tilde{I}_{\phi 3}\right)d_5 - \frac{E\hat{I}_{\phi 2}}{R^2}d_8 \tag{13n}$$

$$+ (\rho\omega^2\tilde{I}_{\phi 2} - GA_{3r})d_9 + \frac{E\hat{I}_{\phi 3}}{R}d_{12} + (\rho\omega^2\tilde{I}_\phi - GA_r)d_{13}$$

Eqs. (13a-n) can be compactly expressed as a following matrix form

$$\boldsymbol{Ad'} = \boldsymbol{Bd} \tag{14}$$

where components of matrices $\boldsymbol{A}$ and $\boldsymbol{B}$ are given in Appendix I.

We consider the following eigenvalue problem with non-symmetric matrix in order to compute the homogeneous solution of the simultaneous differential Eq. (14).

$$\lambda\boldsymbol{AZ} = \boldsymbol{BZ} \tag{15}$$

In this study, IMSL subroutine DGVCRG (IMSL Library 1995) is used to obtain the complex eigensolutions of Eq. (15). From Eq. (15), 14 eigenvalues λ_i and 14×14 eigenvectors $\boldsymbol{Z_i}$ in complex domain can be calculated.

$$(\boldsymbol{\lambda_i}, \boldsymbol{Z_i}), \quad i = 1, 2, \ldots, 14 \tag{16}$$

where

$$\boldsymbol{Z_i} = \langle z_{1i}, z_{2i}, z_{3i}, z_{4i}, z_{5i}, z_{6i}, z_{7i}, z_{8i}, z_{9i}, z_{10i}, z_{11i}, z_{12i}, z_{13i}, z_{14i} \rangle^T \tag{17}$$

Next it is possible that the general solution of Eq. (14) is represented by the linear combination of eigenvectors with complex exponential functions as follows

$$\boldsymbol{d}(\boldsymbol{x}) = \sum_{i=1}^{14} \boldsymbol{a_i} \boldsymbol{Z_i} e^{\lambda_i x} = \boldsymbol{X}(\boldsymbol{x}) \boldsymbol{a} \tag{18}$$

where

$$\boldsymbol{a} = \langle a_1, a_2, a_3, a_4, a_5, a_6, a_7, a_8, a_9, a_{10}, a_{11}, a_{12}, a_{13}, a_{14} \rangle^T \tag{19}$$

$$\begin{aligned}\boldsymbol{X}(\boldsymbol{x}) = [&\boldsymbol{Z}_1 e^{\lambda_1 x};\ \boldsymbol{Z}_2 e^{\lambda_2 x};\ \boldsymbol{Z}_3 e^{\lambda_3 x};\ \boldsymbol{Z}_4 e^{\lambda_4 x};\ \boldsymbol{Z}_5 e^{\lambda_5 x};\ \boldsymbol{Z}_6 e^{\lambda_6 x};\ \boldsymbol{Z}_7 e^{\lambda_7 x};\\ &\boldsymbol{Z}_8 e^{\lambda_8 x};\ \boldsymbol{Z}_9 e^{\lambda_9 x};\ \boldsymbol{Z}_{10} e^{\lambda_{10} x};\ \boldsymbol{Z}_{11} e^{\lambda_{11} x};\ \boldsymbol{Z}_{12} e^{\lambda_{12} x};\ \boldsymbol{Z}_{13} e^{\lambda_{13} x};\ \boldsymbol{Z}_{14} e^{\lambda_{14} x}]\end{aligned} \tag{20}$$

in which $\boldsymbol{a}$ is the integration constant vector and $\boldsymbol{X}(\boldsymbol{x})$ denotes the 14×14 matrix function made up of 14 eigensolutions.

And then it is necessary to represent complex coefficient vector $\boldsymbol{a}$ with respect to 14 nodal displacement components as shown in Fig. 3. For this, the following nodal displacement vector is defined by

$$\boldsymbol{U_e} = \langle \boldsymbol{U^p}, \boldsymbol{U^q} \rangle^T \tag{21a}$$

$$\boldsymbol{U^{\alpha}} = \langle u^{\alpha}, v^{\alpha}, w^{\alpha}, \omega_1^{\alpha}, \omega_2^{\alpha}, \omega_3^{\alpha}, f^{\alpha} \rangle^T, \quad \alpha = p, q \tag{21b}$$

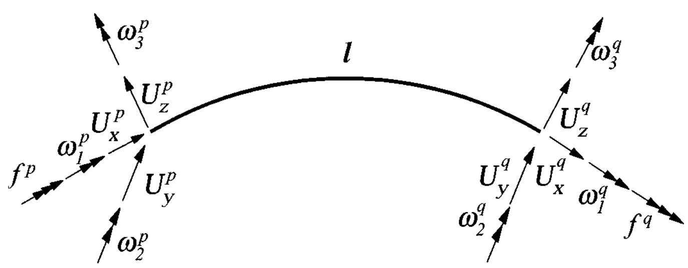

Fig. 3 Nodal displacement vector of a thin-walled curved beam element

where

$$\boldsymbol{U^p} = \langle U_x(o), U_y(o), U_z(o), \omega_1(o), \omega_2(o), \omega_3(o), f(o)\rangle^T \tag{22a}$$

$$\boldsymbol{U^q} = \langle U_x(l), U_y(l), U_z(l), \omega_1(l), \omega_2(l), \omega_3(l), f(l)\rangle^T \tag{22b}$$

The nodal displacement vector $\boldsymbol{U_e}$ is obtained by substituting the coordinates of the member end into Eq. (18) and accounting for Eqs. (22a,b).

$$\boldsymbol{U_e} = \boldsymbol{Ea} \tag{23}$$

where $\boldsymbol{E}$ is evaluated from $\boldsymbol{X}(\boldsymbol{x})$ and the inverse matrix of $\boldsymbol{E}$ is calculated using IMSL subroutine DLINCG (IMSL Library 1995).

Finally elimination of $\boldsymbol{a}$ from Eq. (23) and Eq. (18) yields the exact displacement state vector.

$$\boldsymbol{d}(\boldsymbol{x}) = \boldsymbol{X}(\boldsymbol{x})\boldsymbol{E}^{-1}\boldsymbol{U_e} \tag{24}$$

where $\boldsymbol{X}(\boldsymbol{x})\boldsymbol{E}^{-1}$ denotes the exact interpolation matrix.

3.2 Calculation of dynamic element stiffness matrix

Using the 14 displacement parameters of Eq. (12), force-deformation relations in Eqs. (11a-g) of thin-walled curved beam can be rewritten as

$$F_1 = \left(EA + \frac{E\hat{I}_2}{R^2}\right)d_2 + \frac{E\hat{I}_{23}}{R}d_6 + \left(\frac{EA}{R} + \frac{E\hat{I}_2}{R^3}\right)d_7 - \frac{E\hat{I}_2}{R}d_{10} - \frac{E\hat{I}_{23}}{R^2}d_{11} - \frac{E\hat{I}_{\phi 2}}{R}d_{14} \tag{25a}$$

$$F_2 = -\frac{GA_{23}}{R}d_1 + (GA_2 + {}^oF_1)d_4 - \left(GA_2 - \frac{GA_{2r}}{R}\right)d_5 + GA_{23}d_8 + GA_{23}d_9 + GA_{2r}d_{12} + GA_{2r}d_{13} \tag{25b}$$

$$F_3 = -\frac{1}{R}(GA_3 + {}^oF_1)d_1 + GA_{23}d_4 - \left(GA_{23} - \frac{GA_{3r}}{R}\right)d_5 + (GA_3 + {}^oF_1)d_8 + GA_3d_9 + GA_{3r}d_{12} + GA_{3r}d_{13} \tag{25c}$$

$$\begin{aligned} M_1 = &-\frac{GA_{3r}}{R}d_1 + GA_{2r}d_4 + \left(\frac{GJ}{R} + \frac{GA_r}{R} - GA_{2r} + \frac{\beta_o}{R}{}^oF_1\right)d_5 + GA_{3r}d_8 + GA_{3r}d_9 \\ &+ (GJ + GA_r + \beta^o F_1)d_{12} + GA_r d_{13} \end{aligned} \tag{25d}$$

$$M_2 = -\frac{E\hat{I}_2}{R}d_2 - E\hat{I}_{23}d_6 - \frac{E\hat{I}_2}{R^2}d_7 + E\hat{I}_2 d_{10} + \frac{E\hat{I}_{23}}{R}d_{11} + E\hat{I}_{\phi 2}d_{14} \tag{25e}$$

$$M_3 = \frac{E\hat{I}_{23}}{R}d_2 + E\hat{I}_3 d_6 + \frac{E\hat{I}_{23}}{R^2}d_7 - E\hat{I}_{23}d_{10} - \frac{E\hat{I}_3}{R}d_{11} - E\hat{I}_{\phi 3}d_{14} \tag{25f}$$

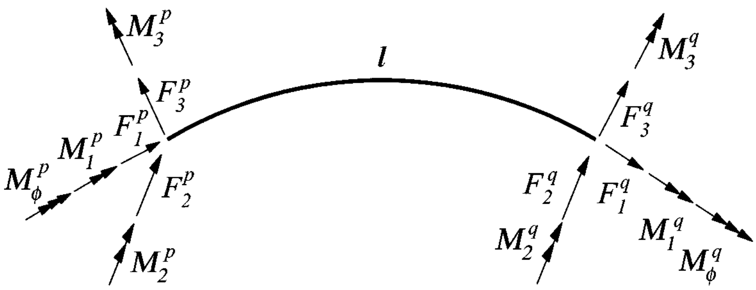

Fig. 4 Nodal force vector of a thin-walled curved beam element

$$M_\phi = -\frac{E\hat{I}_{\phi 2}}{R}d_2 - E\hat{I}_{\phi 3}d_6 - \frac{E\hat{I}_{\phi 2}}{R^2}d_7 + E\hat{I}_{\phi 2}d_{10} + \frac{E\hat{I}_{\phi 3}}{R}d_{11} + E\hat{I}_\phi d_{14} \tag{25g}$$

which equations are compactly represented as a following matrix form

$$\boldsymbol{f}(\boldsymbol{x}) = \boldsymbol{S}\boldsymbol{d}(\boldsymbol{x}) \tag{26}$$

where $\boldsymbol{f} = \langle F_1, F_2, F_3, M_1, M_2, M_3, M_\phi \rangle^T$ and each component of 7×14 matrix $\boldsymbol{S}$ is given in Appendix I.

Substituting Eq. (24) into Eq. (26) leads to

$$\boldsymbol{f}(\boldsymbol{x}) = \boldsymbol{S}\boldsymbol{X}(\boldsymbol{x})\boldsymbol{E}^{-1}\boldsymbol{U}_{\boldsymbol{e}} \tag{27}$$

As shown in Fig. 4, the nodal force vector is defined by

$$\boldsymbol{F}_{\boldsymbol{e}} = \langle \boldsymbol{F}^{\boldsymbol{p}}, \boldsymbol{F}^{\boldsymbol{q}} \rangle^T \tag{28a}$$

$$\boldsymbol{F}^{\boldsymbol{\alpha}} = \langle F_1^\alpha, F_2^\alpha, F_3^\alpha, M_1^\alpha, M_2^\alpha, M_3^\alpha, M_\phi^\alpha \rangle^T, \quad \alpha = p, q \tag{28b}$$

Therefore nodal forces at ends of element (x = 0, l) are evaluated using Eq. (27) as

$$\boldsymbol{F}^{\boldsymbol{p}} = -\boldsymbol{f}(\boldsymbol{o}) = -\boldsymbol{S}\boldsymbol{X}(\boldsymbol{0})\boldsymbol{E}^{-1}\boldsymbol{U}_{\boldsymbol{e}} \tag{29a}$$

$$\boldsymbol{F}^{\boldsymbol{q}} = \boldsymbol{f}(\boldsymbol{l}) = \boldsymbol{S}\boldsymbol{X}(\boldsymbol{l})\boldsymbol{E}^{-1}\boldsymbol{U}_{\boldsymbol{e}} \tag{29b}$$

Consequently the exact dynamic stiffness matrix $\boldsymbol{K}_{\boldsymbol{d}}$ of a spatially coupled shear deformable thin-walled curved beam element with non-symmetric cross section subjected to intial axial forces is evaluated as follows

$$\boldsymbol{F}_{\boldsymbol{e}} = \boldsymbol{K}_{\boldsymbol{d}}\boldsymbol{U}_{\boldsymbol{e}} \tag{30}$$

where

$$\boldsymbol{K}_d = \begin{bmatrix} -\boldsymbol{SX}(\boldsymbol{0})\boldsymbol{E}^{-1} \\ \boldsymbol{SX}(\boldsymbol{l})\boldsymbol{E}^{-1} \end{bmatrix} \tag{31}$$

It should be noted that dynamic stiffness matrix in Eq. (31) is formed by frequency dependent shape functions which are exact solutions of the governing differential equations. Therefore, it eliminates discretization errors and is capable of predicting an infinite number of natural frequencies by means of a finite number of coordinates.

4. Isoparametric and Hermitian curved beam elements

In this section, the isoparametric curved beam element (Kim *et al.* 2004) based on Eqs. (2), (3) and (6) and the Hermitian curved beam element (Kim *et al.* 2002) neglecting shear deformation having an arbitrary thin-walled cross sections are addressed. Fig. 5 shows the nodal displacement vector of a three-noded isoparametric thin-walled beam element with seven nodal degrees of freedom per a node. The coordinate and all the displacement parameters of the beam element can be interpolated with respect to the nodal coordinates and displacements and the elastic stiffness matrix is evaluated using a reduced Gauss numerical integration scheme.

On the other hand, in case of neglecting shear deformation effect, the Hermitian curved beam element with two nodes and eight degrees of freedom per a node as shown in Fig. 6 is used. In

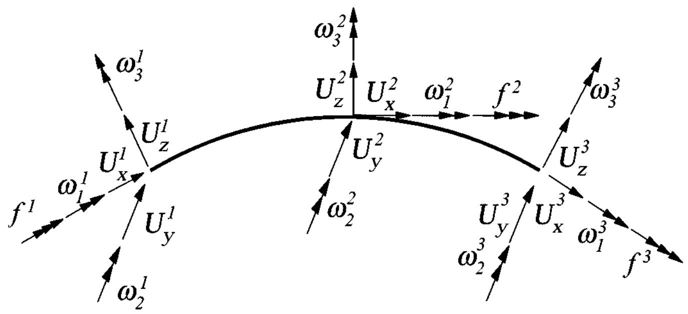

Fig. 5 Nodal displacement vector of a three-noded isoparametric curved beam element

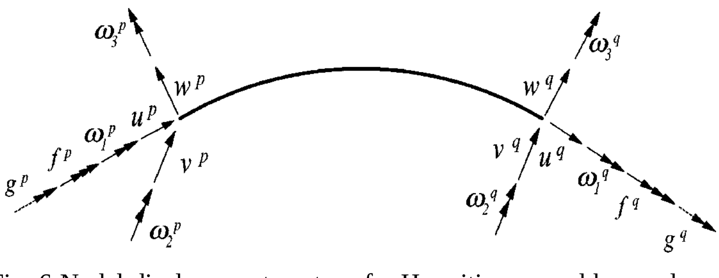

Fig. 6 Nodal displacement vector of a Hermitian curved beam element

order to accurately express the deformation of element, the third order Hermitian polynomials are adopted to interpolate displacement parameters that are defined at the centroid axis.

5. Numerical examples

A wide range of problem can be solved by using the method proposed herein. In numerical examples, the free vibration analysis for the simply supported and clamped curved beams with non-symmetric cross sections are conducted. For verification, the available results from the three-noded isoparametric curved beam elements and the analytic solutions (Kim *et al.* 2004) considering shear deformation effect and the Hermitian curved beam elements (Kim *et al.* 2002) neglecting it are compared in Tables with the current results.

5.1 Simply supported curved beam with x_3 - monosymmetric cross section

Fig. 7 shows the simply supported curved beam with x_3-monosymmetric cross section and its geometric and material data. The beam length l is 100 cm and the subtended angles θ_o for constant length of beam are taken to be 10°, 30°, 60° and 90°, respectively. In this case, the in-plane and the out-of-plane vibration motions are decoupled as one axis of symmetry which lies in the plane of beam curvature. For that reason, we evaluate the lowest three in-plane natural frequencies by this study and present in Table 1. For comparison, FE solutions using 20 three-noded isoparametric curved beam elements (Kim *et al.* 2004) with shear deformation effect and 20 cubic Hermitian curved beam elements (Kim *et al.* 2002) without it are together presented. As can be seen in Table 1, the present solutions using only a single element are in a greatly good agreement with the FE

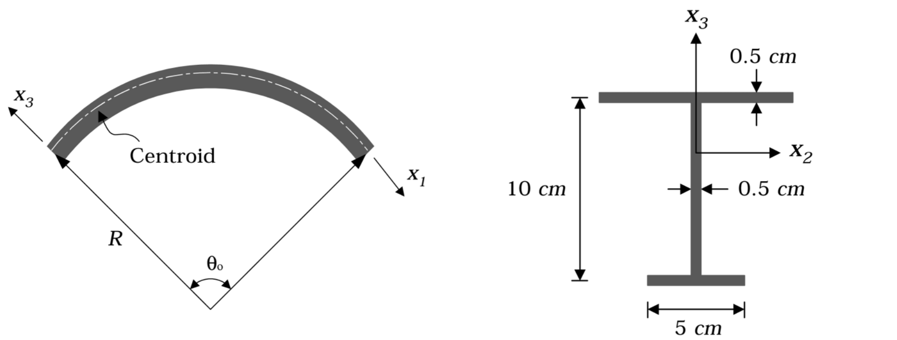

(a) Simply supported curved beam (b) Monosymmetric cross section

$$A = 12.5\,cm^2,\ E = 73{,}000\,N/cm^2,\ G = 28{,}000\,N/cm^2,\ \rho = 0.00785\,N/cm^3,\ J = 1.04167\,cm^4$$

$$e_2 = 0\,cm,\ e_3 = 2.88889\,cm,\ I_2 = 216.66667\,cm^4,\ I_3 = 46.875\,cm^4,\ I_\phi = 485.16667\,cm^6$$

$$I_{\phi 3} = -135.41667\,cm^5,\ I_{222} = -350.0\,cm^5,\ I_{233} = 135.41667\,cm^5,\ I_{\phi\phi 2} = 1541.66667\,cm^7$$

$$I_{\phi 23} = -854.166667\,cm^6,\ A_2^s = 5.11364\,cm^2,\ A_3^s = 4.53387\,cm^2,\ A_r^s = 138.88889\,cm^4$$

(c) Material and section properties

Fig. 7 Simply supported curved beam with x_3 - monosymmetric cross section

Table 1 In-plane natural frequencies of simply supported beam with x_3 - monosymmetric section, ω^2 (rad./sec)^2

Θ_o (degree)	Mode	This study	Finite element method	
			With shear deformation	Without shear deformation
10	1	160.07	160.07	176.41
	2	1629.6	1629.6	2348.6
	3	5831.6	5832.7	9199.5
30	1	334.01	334.01	349.66
	2	1583.6	1583.7	2285.7
	3	5814.9	5816.1	9369.2
60	1	905.40	905.40	926.54
	2	1431.7	1431.8	2071.5
	3	5741.8	5743.0	9915.1
90	1	1216.0	1216.0	1766.9
	2	1786.1	1786.1	1860.5
	3	5681.8	5683.0	10617.

Table 2 Out-of-plane natural frequencies of simply supported beam with x_3 - monosymmetric section, ω^2 (rad./sec)^2

Θ_o (degree)	Mode	This study	Analytic solution	Finite element method	
				With shear deformation	Without shear deformation
10	1	24.694	24.694	24.694	24.966
	2	39.441	39.441	39.441	40.096
	3	207.51	207.51	207.52	215.79
	4	707.26	707.26	707.29	761.91
	5	864.92	864.92	865.13	944.39
30	1	16.805	16.805	16.805	16.980
	2	55.244	55.244	55.244	56.180
	3	260.34	260.34	260.35	270.53
	4	561.13	561.13	561.16	604.40
	5	983.49	983.49	983.71	1076.7
60	1	5.0263	5.0263	5.0263	5.0635
	2	154.92	154.92	154.92	157.97
	3	310.57	310.57	310.59	320.38
	4	455.90	455.90	455.92	494.15
	5	1181.2	1181.2	1181.4	1294.7
90	1	1.6588	1.6588	1.6588	1.6695
	2	228.08	228.08	228.10	237.39
	3	335.34	335.34	335.34	342.17
	4	583.41	583.41	583.42	626.24
	5	1376.2	1376.2	1376.5	1498.6

solutions using the isoparametric beam elements. It should be noticed that the solutions by this study are exact because this curved beam element is based on the exact shape functions which satisfy the element equilibrium equations of motion. Also the FE solutions neglecting shear deformation effect may lead to the erroneous results for the in-plane free vibration of curved beams as the subtended angle increases.

Next, the present lowest five out-of-plane natural frequencies are given in Table 2 with the analytic solutions (Kim *et al.* 2004) and the FE solutions using curved beam elements. From Table 2, it may be seen that the present solutions coincide exactly with the analytical solutions and the influence of shear deformation on the out-of-plane natural frequencies is pronounced at the higher modes.

5.2 Single-span and continuous two-span curved beams with non-symmetric cross section

In this example, we perform the spatially coupled free vibration analysis of simply supported single-span and continuous two-span curved beams with non-symmetric cross section.

First, the single-span curved beam as shown in Fig. 8 is considered, in which the subtended angle

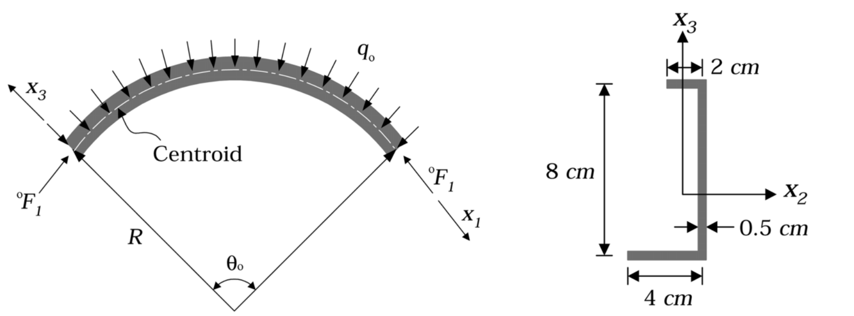

(a) Curved beam subjected to compressive force (b) Non-symmetric cross section

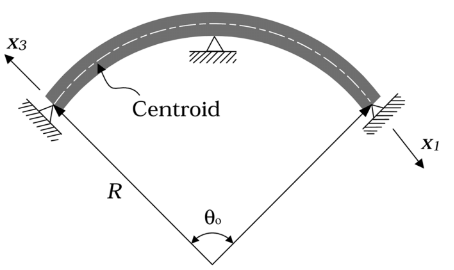

(c) Continuous two-span curved beam

$A = 7.0\,cm^2$, $E = 73000\,N/cm^2$, $G = 28000\,N/cm^2$, $J = 0.5833\,cm^4$, $\rho = 0.00785\,N/cm^3$

$I_2 = 67.0476\,cm^4$, $I_3 = 8.4286\,cm^4$, $I_{23} = 9.1429\,cm^4$, $I_{222} = 52.2449\,cm^5$, $I_{223} = -20.0272\,cm^5$

$I_{233} = -17.4150\,cm^5$, $I_{333} = -13.3878\,cm^5$, $I_\phi = 272.5442\,cm^6$, $I_{\phi 2} = 115.8095\,cm^5$, $I_{\phi 3} = 30.4762\,cm^5$

$I_{\phi 22} = 59.2109\,cm^6$, $I_{\phi 23} = -107.1020\,cm^6$, $I_{\phi 33} = -63.1293\,cm^6$, $I_{\phi\phi 2} = -67.1720\,cm^7$

$I_{\phi\phi 3} = -388.7269\,cm^7$, $A_2^s = 1.69352\,cm^2$, $A_3^s = 3.48152\,cm^2$, $A_r^s = 26.70887\,cm^4$

(d) Material and section properties

Fig. 8 Curved beam with non-symmetric cross section

Table 3 Spatially coupled natural frequencies of simply supported beam with non-symmetric section, ω^2 (rad./sec)^2, (Θ_o = 20^o, F_{cr} = 383.08 N)

Mode	This study	Finite element method			
		4		20	
		With shear deformation	Without shear deformation	With shear deformation	Without shear deformation
1	(5.2850) 10.570 [15.855]	(5.3028) 10.593 [15.883]	(5.3861) 10.670 [15.954]	(5.2850) 10.570 [15.855]	(5.3788) 10.663 [15.947]
2	(119.74) 125.17 [130.61]	(119.90) 125.34 [130.78]	(120.85) 126.28 [131.72]	(119.74) 125.17 [130.61]	(120.83) 126.26 [131.70]
3	(124.63) 145.57 [166.50]	(128.33) 149.58 [170.83]	(129.81) 150.74 [171.66]	(124.64) 145.57 [166.51]	(128.76) 149.68 [170.59]
4	(397.55) 402.93 [408.28]	(398.39) 403.74 [409.07]	(419.86) 425.19 [430.51]	(397.55) 402.93 [408.28]	(419.64) 424.99 [430.32]
5	(570.32) 591.97 [613.61]	(585.05) 607.02 [628.98]	(608.45) 630.12 [651.78]	(570.35) 591.99 [613.64]	(604.66) 626.31 [647.97]
6	(584.21) 631.12 [678.06]	(662.65) 712.89 [763.16]	(645.65) 692.65 [739.67]	(584.35) 631.27 [678.22]	(624.10) 670.94 [717.81]
7	(1683.0) 1766.5 [1850.0]	(2400.8) 2502.2 [2603.6]	(2298.4) 2382.7 [2466.9]	(1684.3) 1767.8 [1851.3]	(1886.0) 1969.1 [2052.3]
8	(2361.0) 2409.5 [2458.0]	(2661.5) 2713.4 [2765.3]	(2765.1) 2813.7 [2862.3]	(2361.5) 2410.1 [2458.6]	(2675.9) 2724.3 [2772.8]
9	(3373.9) 3394.2 [3414.5]	(3459.8) 3480.4 [3501.0]	(4336.5) 4356.2 [4375.9]	(3374.0) 3394.4 [3414.7]	(4304.0) 4323.7 [4343.4]
10	(3769.7) 3899.9 [4030.2]	(8337.2) 8541.6 [8746.0]	(5655.4) 5787.6 [5919.8]	(3776.6) 3906.9 [4037.3]	(4479.4) 4608.8 [4738.2]

Note: ( ) natural frequency with an initial compressive force 191.54 N
[ ] natural frequency with an initial tensile force 191.54 N

θ_o is taken to be 20^o and the beam length is 80 cm. And the initial axial force 191.54 N which is the half value of buckling load F_{cr} is adopted. For the curved beam with non-symmetric cross section, there was no analytic solution reported in previous research for the spatially coupled free vibration. Due to this reason, the lowest ten spatially coupled natural frequencies of curved beam by this study are compared with FE solutions using 4 and 20 isoparametric curved beam elements with shear deformation effect and Hermitian curved beam elements without it in Table 3. Here the

Table 4 Spatially coupled natural frequencies of continuous two-span beam with non-symmetric section, ω^2 (rad./sec)^2, (Θ_o = 20^o)

Mode	This study	Finite element method			
		8		20	
		With shear deformation	Without shear deformation	With shear deformation	Without shear deformation
1	151.10	151.39	155.59	151.11	155.42
2	312.04	313.29	338.22	312.07	337.85
3	635.46	636.53	669.29	635.49	668.31
4	1183.1	1187.5	1368.8	1183.2	1367.2
5	1766.5	1814.3	1982.9	1767.9	1969.2
6	2508.2	2604.0	3084.8	2510.9	3049.9
7	3509.0	3515.0	4450.3	3509.1	4446.5
8	5875.6	5893.5	8116.2	5876.1	8058.1
9	6549.1	6719.8	9612.0	6553.9	9296.0
10	7355.3	8263.3	10359.	7381.7	10345.

parenthesis ( ) and the bracket [ ] denote the natural frequencies subjected to the initial compressive and tensile forces, respectively. From Table 3, it can be found that the natural frequencies obtained from a single element based on the exact dynamic element stiffness matrix are in a excellent agreement with the FE solutions by 20 isoparametric beam elements. Also the method proposed in this study gives exact results in the higher vibrational modes as well as the lower ones, while a large number of beam elements in FE analysis are required to achieve the sufficient accuracy in the higher modes.

Furthermore it is a well recognized fact that the effect of shear deformation decreases the stiffness of curved beam and therefore it decreases the natural frequency of beam. Particularly its effect may be of considerable importance for studying the modes of vibration of higher frequencies when a vibrating curved beam is subdivided by nodal cross sections into comparatively short portions and in this case, the maximum difference is 27.56% at the ninth mode. Also investigation of Table 3 reveals that the effects of initial axial forces on the natural frequencies are predominant in the first few modes and its effect on the fundamental frequency of beam is nearly the same as the ratio of the initial force to the buckling load.

Next, we consider continuous two-span curved beam as shown in Fig. 8(c) which the subtended angle θ_o is 20^o and the total beam length is 80 cm. In this case, the system matrix can be obtained by the usual assembling process from the conditions of equilibrium and compatibility at the nodes. Table 4 shows the spatially coupled natural frequencies by this study using 2 elements and by finite element method with and without shear deformation effect. The excellent agreement between results by this study and 20 isoparametric curved beam elements is evident.

5.3 Clamped curved beam with non-symmetric cross section

In our final example, the spatially coupled free vibration analysis of clamped beam subjected to constant initial axial force is performed. The cross section of beam is the same as previous example

Table 5 Spatially coupled natural frequencies of clamped beam with non-symmetric section, ω^2 (rad./sec)^2, (Θ_o = 20^o, F_{cr} = 1519.7N)

Mode	This study	Finite element method			
		4		20	
		With shear deformation	Without shear deformation	With shear deformation	Without shear deformation
1	(27.699) 53.751 [78.808]	(28.276) 54.224 [79.242]	(29.929) 56.225 [81.878]	(27.700) 53.752 [78.809]	(29.577) 55.928 [81.465]
2	(201.71) 227.76 [253.52]	(203.15) 229.15 [254.88]	(216.16) 242.95 [269.58]	(201.71) 227.76 [253.53]	(213.85) 240.52 [267.00]
3	(209.39) 304.08 [397.32]	(226.00) 321.73 [416.15]	(238.29) 335.62 [432.49]	(209.42) 304.11 [397.35]	(233.13) 329.87 [425.52]
4	(822.00) 1021.7 [1170.6]	(1027.6) 1157.3 [1184.1]	(1000.2) 1213.6 [1422.3]	(822.39) 1022.1 [1170.7]	(959.05) 1164.0 [1365.1]
5	(1049.5) 1145.5 [1232.1]	(1111.0) 1208.1 [1304.9]	(1257.0) 1357.8 [1458.5]	(1049.6) 1145.6 [1232.5]	(1234.0) 1334.0 [1433.7]
6	(1131.2) 1156.8 [1241.1]	(1141.5) 1250.2 [1461.2]	(1542.7) 1571.0 [1604.2]	(1131.2) 1156.8 [1241.3]	(1533.6) 1561.7 [1593.1]
7	(2160.4) 2507.7 [2854.3]	(3620.3) 4037.6 [4453.8]	(3708.4) 4097.6 [4487.1]	(2162.9) 2510.4 [2857.1]	(2691.8) 3049.8 [3407.6]
8	(3556.5) 3760.6 [3964.5]	(4293.8) 4511.0 [4728.0]	(4790.8) 5013.1 [5235.4]	(3557.9) 3762.1 [3966.0]	(4595.1) 4808.7 [5022.1]
9	(4535.0) 5067.5 [5599.3]	(5898.7) 5987.0 [6075.9]	(10216.) 10332. [10420.]	(4546.2) 5079.2 [5611.6]	(6065.3) 6613.8 [7162.1]
10	(5649.2) 5736.5 [5823.3]	(12376.) 13186. [13917.]	(10243.) 10851. [11486.]	(5649.7) 5737.0 [5823.8]	(10047.) 10135. [10222.]

Note: ( ) natural frequency with an initial compressive force 759.85 N
[ ] natural frequency with an initial tensile force 759.85 N

and the subtended angle and the beam length are 20^o and 80 cm, respectively. Here the initial axial force 759.85 N is acted along the clamped beam which is the half value of buckling load. The lowest ten natural frequencies by this study using a single element are compared with FE solutions using 4 and 20 curved beam elements with and without shear deformation effect in Table 5. The excellent agreement between results by this study and 20 isoparametric curved beam elements can

Table 6 Spatially coupled natural frequencies of clamped beam with non-symmetric section, ω (rad./sec), (Θ_o = 30°)

Mode	This study	Finite element method (with shear deformation)		ABAQUS
		4	20	
1	2.4053	2.4189	2.4053	2.4193
2	5.8512	6.0299	5.8515	5.8867
3	7.2931	7.3061	7.2932	7.2632
4	10.612	11.658	10.614	10.717
5	11.597	11.879	11.597	11.698
6	13.325	13.484	13.325	13.255
7	16.734	21.552	16.743	16.971
8	20.701	22.738	20.705	20.937
9	23.958	27.914	23.988	24.271
10	27.189	40.876	27.190	26.450

be observed from Table 5. Also the shear deformation effect increases up to the maximum difference 77.83% at the tenth mode.

Next the clamped curved beam with the subtended angle 30° and the beam length 80 cm is considered. In Table 6, the spatially coupled natural frequencies by this study are presented. For comparison, FE solutions with shear deformation effect and the results obtained from 300 nine-noded shell elements (S9R5) of ABAQUS which is the commercial finite element analysis program are given. Where a good agreement between results by this study and ABAQUS is observed with less than 2.8% as maximum of difference at the tenth mode.

6. Conclusions

For the spatially coupled free vibration analysis of shear deformable thin-walled curved beams with non-symmetric cross section subjected to intial axial force, an effective method evaluating the exact dynamic element stiffness matrix is developed in this study.

Through the numerical examples, it is demonstrated that results by the present method using only a single element are in a great agreement with those by thin-walled curved beam elements and ABAQUS's shell elements. Also the influence of shear deformation and the intial axial force on the spatially coupled vibrational behavior of curved beams is investigated.

As a result, it is believed that this procedure is general enough to provide a systematic tool for exact solutions of simultaneous ordinary differential equations of the higher order with constant coefficients. Furthermore, the exact curved beam element eliminates discretization errors and is capable of predicting an infinite number of natural frequencies of shear deformable curved beams by means of a finite number of coordinates.

Acknowledgements

This paper was supported by Samsung research fund, Sungkyunkwan University 2000 and Korea Ministry of Construction & Transportation through Korea Bridge Design & Engineering Research Center at Seoul National University. The authors wish to express their gratitude for the financial support.

References

Eisenberger, M. and Efraim, E. (2001), "In-plane vibrations of shear deformable curved beams", *Int. J. Numer. Meth. Eng.*, **52**, 1221-1234.

Gupta, A.K. and Howson, W.P. (1994), "Exact natural frequencies of plane structures composed of slender elastic curved members", *J. Sound Vib.*, **175**, 145-157.

Howson, W.P. and Jemah, A.K. (1999), "Exact dynamic stiffness method for planar natural frequencies of curved Timoshenko beams", *Proc. Instn Mech. Engrs.*, **213**, 687-696.

Howson, W.P. and Jemah, A.K. (1999), "Exact out-of-plane natural frequencies of curved Timoshenko beams", *J. Eng. Mech.*, **125**, 19-25.

Howson, W.P., Jemah, A.K. and Zhou, J.Q. (1995), "Exact natural frequencies for out-of-plane motion of plane structures composed of curved beam members", *Comput. Struct.*, **55**, 989-995.

Huang, C.S., Tseng, Y.P. and Chang, S.H. (1998), "Out-of-plane dynamic responses of non-circular curved beams by numerical Laplace transform", *J. Sound Vib.*, **215**, 407-424.

Huang, C.S., Tseng, Y.P., Chang, S.H. and Hung, C.L. (2000), "Out-of-plane dynamic analysis of beams with arbitrarily varying curvature and cross-section by dynamic stiffness matrix method", *Int. J. Solids Struct.*, **37**, 495-513.

Huang, C.S., Tseng, Y.P., Leissa, A.W. and Nieh, K.Y. (1998), "An exact solution for in-plane vibrations of an arch having variable curvature and cross section", *Int. J. Mech. Sci.*, **40**, 1159-1173.

Kang, K., Bert, C.W. and Striz, A.G. (1995), "Vibration analysis of shear deformable circular arches by the differential quadrature method", *J. Sound Vib.*, **181**, 353-360.

Kang, K., Bert, C.W. and Striz, A.G. (1996), "Vibration analysis of horizontally curved beams with warping using DQM", *J. Struct. Eng.*, **215**, 657-662.

Kang, K., Bert, C.W. and Striz, A.G. (1996), "Vibration and buckling analysis of circular arches using DQM", *Comput. Struct.*, **60**, 49-57.

Kim, M.Y., Kim, N.I. and Min, B.C. (2002), "Analytical and numerical study on spatial free vibration of non-symmetric thin-walled curved beams", *J. Sound Vib.*, **258**, 595-618.

Kim, M.Y., Min, B.C. and Suh, M.W. (2000), "Spatial stability of nonsymmetric thin-walled curved beams. I: Analytical approach", *J. Eng. Mech.*, **126**, 497-504.

Kim, N.I. and Kim, M.Y. (2004), "Spatial free vibration of shear deformable circular curved beams with non-symmetric thin-walled sections", *J. Sound Vib.*, **276**, 245-271.

Lee, S.Y. and Chao, J.C. (2001), "Exact solutions for out-of-plane vibration of curved nonuniform beams", *J. Appl. Mech.*, **68**, 186-191.

Microsoft IMSL Library 1995, Microsoft Corporation.

Nieh, K.Y., Huang, C.S. and Tseng, Y.P. (2003), "An analytical solution for in-plane vibration and stability of loaded elliptic arches", *Comput. Struct.*, **81**, 1311-1327.

Tseng, Y.P., Huang, C.S. and Lin, C.J. (1997), "Dynamic stiffness analysis for in-plane vibrations of arches with variable curvature", *J. Sound Vib.*, **207**, 15-31.

Whittaker, E.T. and Watson, G.N. (1965), *A Course of Modern Analysis*. Cambridge: Cambridge University Press; fourth edition.

Wittrick, W.H. and Williams, F.W. (1971), "A general algorithm for computing natural frequencies of elastic structures", *Quarterly J. Mech. Appl. Mathematics*, **24**, 263-284.

Yildrim, V. (1997), "A computer program for the free vibration analysis of elastic arcs", *Comput. Struct.*, **78**, 475-485.

Appendix I. Each components of matrices *A*, *B* and *S*

1) Components of matrix A

$$
\left[\begin{array}{ccccccc|ccccccc}
k_1 & & & & & & & & & & & & & \\
 & k_2 & k_3 & & & k_4 & k_5 & & & k_6 & k_7 & & & k_8 \\
 & & k_1 & & & & & & & & & & & \\
 & & & k_9 & & & & k_{10} & & & & k_{11} & & \\
 & & & & k_1 & & & & & & & & & \\
k_{12} & & & -k_{10} & k_{13} & & & k_{14} & k_{15} & & & k_{16} & & \\
 & & & & & & k_1 & & & & & & & \\
\hline
k_{17} & & & -k_{11} & k_{18} & & & k_{16} & -k_4 & & & k_{19} & & \\
 & & & & & & & & k_1 & & & & & \\
 & k_6 & k_{10} & & & k_{20} & k_{21} & & & k_{22} & -k_{16} & & & k_{23} \\
 & & & & & & & & & & k_1 & & & \\
 & k_4 & k_{24} & & & k_{25} & k_{26} & & & k_{20} & k_{27} & & & k_{28} \\
 & & & & & & & & & & & & k_1 & \\
 & k_8 & k_{11} & & & k_{28} & -k_{16} & & & k_{23} & k_{29} & & & k_{30}
\end{array}\right] \tag{A-1}
$$

where

$$k_1 = 1.0, \quad k_2 = -EA - \frac{E\hat{I}_2}{R^2}, \quad k_3 = -\frac{GA_{23}}{R}, \quad k_4 = -\frac{E\hat{I}_{23}}{R}, \quad k_5 = -\frac{GA_3}{R},$$

$$k_6 = \frac{E\hat{I}_2}{R}, \quad k_7 = -\frac{GA_{3r}}{R}, \quad k_8 = \frac{E\hat{I}_{\phi 2}}{R}, \quad k_9 = GA_2 + {}^oF_1, \quad k_{10} = GA_{23}, \quad k_{11} = GA_{2r},$$

$$k_{12} = \frac{1}{R}\left(EA + \frac{E\hat{I}_2}{R^2} + GA_3 + {}^oF_1\right), \quad k_{13} = \frac{E\hat{I}_{23}}{R^2}, \quad k_{14} = -(GA_3 + {}^oF_1), \quad k_{15} = -\frac{E\hat{I}_2}{R^2},$$

$$k_{16} = -GA_{3r}, \quad k_{17} = -\frac{1}{R}\left(\frac{E\hat{I}_{23}}{R} - GA_{3r}\right), \quad k_{18} = -\frac{1}{R}(E\hat{I}_3 + GA_r), \quad k_{19} = -GJ - GA_r - \beta^oF_1,$$

$$k_{20} = E\hat{I}_{23}, \quad k_{21} = GA_3, \quad k_{22} = -E\hat{I}_2, \quad k_{23} = -E\hat{I}_{\phi 2}, \quad k_{24} = -GA_2 + \frac{GA_{2r}}{R}, \quad k_{25} = -E\hat{I}_3,$$

$$k_{26} = -GA_{23} + \frac{GA_{3r}}{R}, \quad k_{27} = \frac{GJ}{R} + \frac{GA_r}{R} - GA_{2r} + \frac{\beta}{R}{}^oF_1, \quad k_{28} = E\hat{I}_{\phi 3}, \quad k_{29} = GA_r, \quad k_{30} = -E\hat{I}_{\phi}$$

2) Components of matrix B

$$
\left[\begin{array}{ccccccc|ccccccc}
 & b_1 & & & & & & & & & & & & \\
b_2 & & & & b_3 & & & b_4 & b_5 & & & b_6 & b_7 & \\
 & & & b_1 & & & & & & & & & & \\
 & b_8 & b_9 & & & b_{10} & & & & b_{11} & b_{12} & & & b_{13} \\
 & & & & & b_1 & & & & & & & & \\
 & & & & & b_{14} & b_{15} & & & b_{16} & b_{17} & & & b_{18} \\
 & & & & & & & b_1 & & & & & & \\
\hline
 & & -b_{12} & & & b_{19} & b_{17} & & & b_{20} & b_{21} & & & b_{22} \\
 & & & & & & & & & b_1 & & & & \\
b_5 & & & & b_{23} & & & b_{24} & b_{25} & & & b_{26} & b_{27} & \\
 & & & & & & & & & & & b_1 & & \\
 & b_3 & & & b_{28} & & & -b_6 & b_{23} & & & b_{29} & b_{30} & \\
 & & & & & & & & & & & & & b_1 \\
b_7 & & & & b_{30} & & & b_{31} & b_{27} & & & b_{32} & b_{33} &
\end{array}\right] \tag{A-2}
$$

where

$$b_1 = 1.0, \quad b_2 = -\frac{1}{R^2}(GA_3 + {}^oF_1) + \rho\omega^2 A, \quad b_3 = -\frac{GA_{23}}{R} + \frac{GA_{3r}}{R^2} - \rho\omega^2\frac{I_{23}}{R},$$

$$b_4 = \frac{1}{R}\left(EA + \frac{E\hat{I}_2}{R^2} + {}^oF_1\right), \quad b_5 = \frac{GA_3}{R} + \rho\omega^2\frac{I_2}{R}, \quad b_6 = -\frac{E\hat{I}_{23}}{R^2}, \quad b_7 = \frac{GA_{3r}}{R} + \rho\omega^2\frac{I_{\phi 2}}{R},$$

$$b_8 = \frac{GA_{23}}{R}, \quad b_9 = -\rho\omega^2 A, \quad b_{10} = GA_2 - \frac{GA_{2r}}{R}, \quad b_{11} = -GA_{23}, \quad b_{12} = \rho\omega^2\frac{I_2}{R}, \quad b_{13} = -GA_{2r},$$

$$b_{14} = -GA_{23} + \frac{GA_{3r}}{R}, \quad b_{15} = -\frac{1}{R^2}\left(EA + \frac{E\hat{I}_2}{R^2}\right) + \rho\omega^2 A, \quad b_{16} = GA_3, \quad b_{17} = \frac{E\hat{I}_{23}}{R^3} + \rho\omega^2\frac{I_{23}}{R},$$

$$b_{18} = GA_{3r} + \frac{E\hat{I}_{\phi 2}}{R^2}, \quad b_{19} = \frac{GJ}{R} - GA_{2r} + \frac{\beta_o}{R}{}^oF_1, \quad b_{20} = GA_{3r}, \quad b_{21} = -\frac{E\hat{I}_3}{R^2} + \rho\omega^2\tilde{I}_o,$$

$$b_{22} = -\frac{E\hat{I}_{\phi 3}}{R} + GA_r, \quad b_{23} = GA_{23} - \frac{GA_{3r}}{R} - \rho\omega^2\tilde{I}_{23}, \quad b_{24} = -\frac{E\hat{I}_2}{R^2}, \quad b_{25} = -GA_3 + \rho\omega^2\tilde{I}_2,$$

$$b_{26} = \frac{E\hat{I}_{23}}{R}, \quad b_{27} = -GA_{3r} + \rho\omega^2\tilde{I}_{\phi 2}, \quad b_{28} = -\frac{GJ}{R^2} - GA_2 - \frac{GA_r}{R^2} + \frac{2GA_{2r}}{R} - \frac{\beta_o}{R^2}{}^oF_1 + \rho\omega^2\tilde{I}_{\phi 3},$$

$$b_{29} = -\frac{E\hat{I}_3}{R}, \quad b_{30} = -\frac{GA_r}{R} + GA_{2r} - \rho\omega^2\tilde{I}_{\phi 3}, \quad b_{31} = -\frac{E\hat{I}_{\phi 2}}{R^2}, \quad b_{32} = -\frac{E\hat{I}_{\phi 3}}{R}, \quad b_{33} = -GA_r + \rho\omega^2\tilde{I}_{\phi}$$

3) Components of matrix S

$$
\left[\begin{array}{ccccccc|ccccccc}
 & s_1 & & & & s_2 & s_3 & & & s_4 & s_5 & & & s_6 \\
s_7 & & & s_8 & s_9 & & & s_{10} & s_{10} & & & s_{11} & s_{11} & \\
s_{12} & & & s_{10} & s_{13} & & & s_{14} & s_{15} & & & s_{16} & s_{16} & \\
s_{17} & & & s_{11} & s_{18} & & & s_{16} & s_{16} & & & s_{19} & s_{20} & \\
 & s_4 & & & & s_{21} & s_{22} & & & s_{23} & s_2 & & & s_{24} \\
 & s_2 & & & & s_{25} & -s_5 & & & s_{21} & s_{26} & & & s_{27} \\
 & s_6 & & & & s_{27} & s_{28} & & & s_{24} & s_{29} & & & s_{30}
\end{array}\right] \tag{A-3}
$$

where

$$s_1 = EA + \frac{E\hat{I}_2}{R^2}, \quad s_2 = \frac{E\hat{I}_{23}}{R}, \quad s_3 = \frac{1}{R}\left(EA + \frac{E\hat{I}_2}{R^2}\right), \quad s_4 = -\frac{E\hat{I}_2}{R}, \quad s_5 = -\frac{E\hat{I}_{23}}{R^2},$$

$$s_6 = -\frac{E\hat{I}_{\phi 2}}{R}, \quad s_7 = -\frac{GA_{23}}{R}, \quad s_8 = GA_2 + {}^oF_1, \quad s_9 = -GA_2 + \frac{GA_{2r}}{R}, \quad s_{10} = GA_{23}, \quad s_{11} = GA_{2r},$$

$$s_{12} = -\frac{1}{R}(GA_3 + {}^oF_1), \ \ s_{13} = -GA_{23} + \frac{GA_{3r}}{R}, \quad s_{14} = GA_3 + {}^oF_1, \quad s_{15} = GA_3, \quad s_{16} = GA_{3r},$$

$$s_{17} = -\frac{GA_{3r}}{R}, \quad s_{18} = \frac{GJ}{R} + \frac{GA_r}{R} - GA_{2r} + \frac{\beta_o}{R}F_1, \ \ s_{19} = GJ + GA_r + \beta^o F_1, \ \ s_{20} = GA_r,$$

$$s_{21} = -E\hat{I}_{23}, \ \ s_{22} = -\frac{E\hat{I}_2}{R^2}, \ \ s_{23} = E\hat{I}_2, \ \ s_{24} = E\hat{I}_{\phi 2}, \ \ s_{25} = E\hat{I}_3, \ \ s_{26} = -\frac{E\hat{I}_3}{R^2},$$

$$s_{27} = -E\hat{I}_{\phi 3}, \quad s_{28} = -\frac{E\hat{I}_{\phi 2}}{R^2}, \quad s_{29} = \frac{E\hat{I}_{\phi 3}}{R}, \ \ s_{30} = E\hat{I}_\phi$$